Research article

Jingjing Guo*, Bingqian Zhou, Zhou Du, Changxi Yang, Lingjie Kong* and Lijun Xu

Soft and plasmonic hydrogel optical probe for glucose monitoring

https://doi.org/10.1515/nanoph-2021-0360
Received July 9, 2021; accepted August 21, 2021;
published online September 2, 2021

Abstract: Glucose monitoring sensors with high softness and flexibility are critical for the developments of wearable and implantable healthcare devices that enable diagnosis, prognosis, and management of diabetes. The design and implementation of such sensors have been extensively exploited by electrochemical strategies, which, however, suffer from poor reusability and complex modification procedures, and necessitate frequent calibration or sensor replacement due to enzymatic reaction instability. Here, a soft and plasmonic hydrogel optical sensor is created for quantitative and continuous glucose monitoring under physiological conditions. The optical sensor consists of a flexible optical fiber made from composites of gold nanoparticles and glucose-responsive hydrogels. The reversible binding of glucose to the nanocomposite optical fiber results in dynamic volume expansion of the hydrogel matrix, which modulates the localized surface plasmon resonance effect, enabling glucose to be quantified from the light transmission. To achieve robust readout, a dual-wavelength differential approach is employed to endow the sensor with self calibration capability. We show that the sensor is reversible and reusable for detecting physiological glucose levels with high linearity and negligible hysteresis. The soft and flexible glucose sensor holds great promises of serving as a minimally-invasive probe for point-of-care glucose monitoring in clinics.

Keywords: hydrogel optical fiber; nanocomposite; optical devices; optical glucose sensors.

***Corresponding authors: Jingjing Guo**, School of Instrumentation and Optoelectronic Engineering, Beihang University, Beijing 100191, China; and Beijing Advanced Innovation Center for Big Data-Based Precision Medicine, Interdisciplinary Innovation Institute of Medicine and Engineering, Beihang University, Beijing 100191, China; and **Lingjie Kong**, State Key Laboratory of Precision Measurement Technology and Instruments, Department of Precision Instruments, Tsinghua University, Beijing 100084, China,
E-mail: guojj13@buaa.edu.cn (J. Guo), konglj@tsinghua.edu.cn (L. Kong). https://orcid.org/0000-0002-3893-2319 (J. Guo), https://orcid.org/0000-0002-8250-7547 (L. Kong)
Bingqian Zhou and Changxi Yang, State Key Laboratory of Precision Measurement Technology and Instruments, Department of Precision Instruments, Tsinghua University, Beijing 100084, China
Zhou Du, Department of Toxicology and Sanitary Chemistry, School of Public Health, Capital Medical University, Beijing 100069, China
Lijun Xu, School of Instrumentation and Optoelectronic Engineering, Beihang University, Beijing 100191, China; and Beijing Advanced Innovation Center for Big Data-Based Precision Medicine, Interdisciplinary Innovation Institute of Medicine and Engineering, Beihang University, Beijing 100191, China

1 Introduction

Diabetes is a chronic and incurable disease indicated by elevated levels of blood glucose due to insulin deficiency [1]. If left uncontrolled, high levels of blood glucose could lead to serious diabetes complications including kidney failure, heart attack, nerve damage, and vision loss [2, 3]. Therefore, continuous monitoring and tight control of blood glucose level are of great significance in effectively managing diabetes and reducing the risk of complications. In clinics, the concentration of blood glucose is generally monitored by performing finger-stick tests several times a day, which are invasive and painful, resulting in low patient compliance [4, 5]. To address the clinical issue, implantable glucose sensors based on electrochemical strategies have been developed for real-time and continuous glucose measurements, which can be combined with insulin pumps to automatically manage insulin infusion in diabetes therapy [6–9]. However, these sensors often suffer from the limitation of short lifetime and poor biocompatibility, which hinder their applications for long-term *in vivo* glucose motoring [10]. Moreover, the instability of enzymatic reactions could lead to serious signal drift of the electrochemical sensors, which necessitate frequent calibration or replacement [11, 12].

To address above limitations, there have been tremendous attempts to quantify glucose concentration by using minimally-invasive optical fiber probes, which provide real-time measurements over long periods with miniaturized size, built-in calibration, and electromagnetic interference (EMI)

immunity [13–21]. For glucose sensing, a common strategy is to incorporate the tip of optical fibers with functionalized micro and nanostructures such as interferometric cavity [14–16], fluorophores [17, 18], and plasmonic nanoparticles [19–21]. For example, Tierney et al. incorporated a glucose-responsive coating layer at the end of an optical fiber to form a Fabry–Perot cavity, which enabled sensitive glucose readout from the changes of the cavity length [15]. Liao et al. demonstrated a percutaneous and disposable fiber-optic sensor by coating the fiber tip with a fluorophores-assembled polymeric matrix for long-term glucose monitoring *in vivo* [17]. However, the practical applications of fiber-optic sensors in clinics are hindered by poor biocompatibility of the fiber materials, and fragile nature of the fiber tip [22, 23]. Moreover, the high stiffness of conventional optical fibers (e.g., silica and plastics) may easily cause tissue lesions during implantation or body movements.

Polymeric hydrogels have been intensively investigated as promising candidates for bio-optical sensing due to their exceptional optical and physico-mechanical properties [24–26]. Many synthetic hydrogels, such as polyethylene glycol diacrylate (PEGDA), polyacrylamide (PAAm), and poly(vinyl alcohol) (PVA), have been utilized to fabricate optical waveguides with high softness and biocompatibility for implantable and biomedical applications [27–34]. For example, hydrogel optical fibers composed of a PEGDA core and an alginate cladding were implanted in living mice for blood oxygenation sensing [29]. Low-modulus and stretchable alginate-PAAm hydrogel optical fibers were demonstrated for optogenetic brain modulation in free-moving mice [33]. The hydrogel-based optical waveguide offers a versatile platform that enables the incorporation of active recognition motif or functionalized nanostructures into the hydrogel matrix to meet the demands in diverse biosensing and biomedical applications [35–42]. Recently, hydrogel optical fibers involving phenylboronic acid (PBA) derivatives have been reported for continuous glucose monitoring, in which glucose concentration was detected from the changes in transmitted light intensities induced by the volumetric changes [43]. However, the detection of glucose directly from light intensity suffers from a variety of potential interferences such as the intensity fluctuation of light source, changes of the surrounding environments, and light loss associated with fiber deformation, which poses practical challenges for precise quantification of glucose. The development of minimally invasive hydrogel optical probe with robust and continuous glucose readout can offer attractive building blocks for better glucose control in diabetes care.

Here, we present a soft and flexible optical glucose sensor with self calibrated differential readout for quantitative and continuous glucose monitoring under physiological conditions. The optical sensor was made of a biocompatible hydrogel optical fiber incorporating covalently immobilized gold nanoparticles (GNPs). To achieve glucose responsivity, the nanocomposite hydrogel fiber was functionalized with 3-(acrylamido)-phenylboronic acid (3-APBA), which possesses a high binding affinity to glucose molecules. The complexation of 3-APBA with glucose molecules increased the boronate anions and Donnan osmotic pressure in the hydrogel matrix, resulting in volume expansion of the fiber. This volumetric change modulated the localized surface plasmon resonance (LSPR) effect of the nanocomposite fiber, enabling quantitative glucose measurements from the transmitted light attenuation at the LSPR peak. To minimize the LSPR-independent loss effects such as fiber bending, a dual-wavelength differential approach was employed for the sensor readout, where a reference wavelength out of the plasmon resonance was introduced to provide an internal calibration. Glucose quantification tests were performed, which demonstrated a reversible and linear response of the sensor with fast readout rate in physiological ranges.

2 Results and discussion

Glucose-responsive hydrogel optical fibers were fabricated from the 3-APBA functionalized PAAm hydrogel by molding and UV-induced photo-crosslinking (Figure 1a). Hydrogel precursor was injected into a poly(vinyl chloride) (PVC) tube mold, followed by UV irradiation for crosslinking. Demolding of the hydrogel fiber from the PVC tube was achieved by water pressure. For LSPR sensing, carboxylic acid-modified GNPs were covalently incorporated into the polymer matrix through EDC conjunction at pH 4.5. Figure 1b shows the photographs of the fabricated hydrogel fibers with/without GNPs doping. In contrast to the transparent undoped fiber, the GNPs-doped fiber showed up in light red as result of the absorption and scattering of light by the nanomaterials (Figure 1b). Transmission electron microscope (TEM) image revealed uniform size (~17.2 nm in average) and morphology of the GNPs (Figure 1c). To evaluate the optical performances, green laser at 532 nm was coupled to the fiber through an objective lens. The fiber could efficiently guide light even when tied into knots or transmitted through mediums of different refractive indices, as confirmed from the bright light spot at the fiber end (Figure 1d,e). The light-guiding capability of the hydrogel fiber suggests its potentials of serving as a flexible optical implant to deliver light to target tissue for

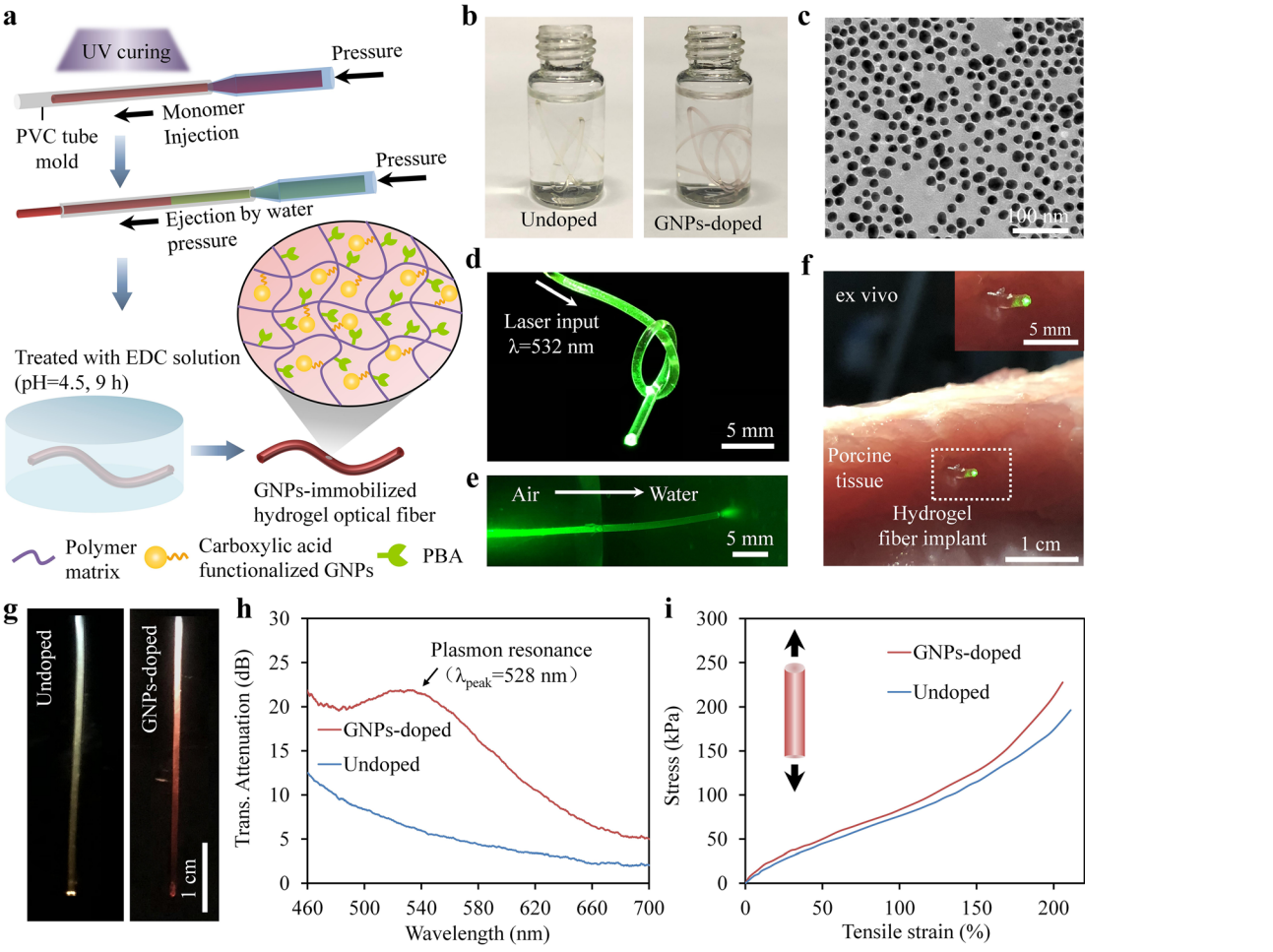

Figure 1: (a) Fabrication of the gold nanocomposite hydrogel optical fibers. (b) Photographs of the hydrogel fibers with/without gold nanoparticles (GNPs) doping. (c) Transmission electron microscope (TEM) image of the GNPs. (d) A hydrogel fiber guides light at 532 nm when tied into knot. (e) Light guiding from the air to water. (f) Implantation of the hydrogel fibers for deep-tissue light delivery. (g) Photographs of the hydrogel fibers when illuminated by a white light source. Left: undoped; Right: GNPs-doped. (h) Transmission spectra. (i) Results of tensile test.

biosensing and light-activated therapy applications. For demonstrations, we implanted the hydrogel fiber inside a porcine tissue at 4 cm depth with the aid of a gauge needle, where the implanted fiber showed confined light through tissue (Figure 1f). Transmission spectra of the fibers were further investigated by illuminating them with a white light source (Figure 1g). The undoped fiber exhibited decreased optical loss with the increasing wavelength due to the light scattering from structural inhomogeneity and surface roughness (Figure 1h). Incorporation of the GNPs within the hydrogel fiber resulted in a notable absorption peak at 528 nm, corresponding to the SPR of the GNPs.

For implantable and subcutaneous glucose monitoring, the soft and elastic nature of the biological tissues required the sensing fibers to be highly flexible and stretchable so that they could endure large mechanical deformations during body motions, and conformally interact with the target tissues. The Young's modulus of human skin tissues is in the range of 0.1–2 MPa, and the stretchability is 30–70% [44]. In contrast, a standard silica optical fiber has a Young's modulus of ~70 GPa, five orders of magnitudes higher than that of skin tissues [45]. Besides, the stretchability of silica fibers is less than 1%. Due to its significant mismatch in mechanical properties with soft tissues, subcutaneously-implanted silica fiber could easily cause the host tissue injuries, which may subsequently lead to chronic inflammation, swelling, and pain at the implant sites [46]. Hydrogel-based optical fibers are promising candidates to address the above limitations. We characterized the mechanical properties of the fabricated hydrogel fibers by tensile testing (Figure 1i). The undoped fiber possessed a high stretchability of ~210%, failure

stress of 196.3 kPa, and a low Young's modulus of 116.9 kPa, compatible with the soft skin tissues. Moreover, the incorporation of GNPs into the hydrogel matrix did not significantly influence its mechanical properties. The GNPs-doped nanocomposite fiber showed a similar stretchability (~205%), but slightly increased mechanical strength (227.9 kPa) and Young's Modulus (145.2 kPa) in comparison with the undoped fiber. The high softness and stretchability of the fibers make them particularly promising for potential clinical applications.

We applied the gold nanocomposite hydrogel fiber for glucose sensing through reversible complexation of the immobilized 3-APBA in the hydrogel matrix with the glucose molecules (Figure 2a). Light transmitted through the nanocomposite fiber was scattered and absorbed by the incorporated GNPs, causing light attenuation. Glucose molecules could easily penetrate into the fiber through passive diffusion and bind with the boronic acid groups. The binding process increased the boronate anions and Donnan osmotic pressure in the fiber, resulting in swelling of the hydrogel matrix [47]. This glucose-dependent volumetric shift could be observed as a change in the light attenuation contributed by the LSPR effect, enabling quantitative glucose measurements (Figure 2b). As the hydrogel swells upon binding with glucose, the volume of the fiber increased, but the amount of incorporated GNPs was kept unchanged due to the strong covalent attachment of GNPs to the hydrogel matrix. As a result, the concentration of GNPs would decrease with the fiber expansion, leading to decreased light attenuation at the LSPR peak.

The dynamic swelling behaviors of the nanocomposite fibers in response to glucose were investigated by optical microscopy. The fibers were fully swollen in phosphate-buffered saline (PBS) (pH = 7.4) prior to the test. Figure 3a and b shows time-lapse microscope images of the nanocomposite fibers in the absence and presence of glucose, respectively. As expected, no expansion of the fibers was observed in the absence of glucose. When exposed to glucose solution (pH = 7.4, 30 mM), the fibers showed 6% expansion in diameter over 60 min due to the specific 3-APBA-glucose binding. We further examined the influence of 3-APBA concentrations on swelling kinetics of the fibers, for which the swelling weight ratio of the fibers was measured (Figure 3c). The weights of the fibers were

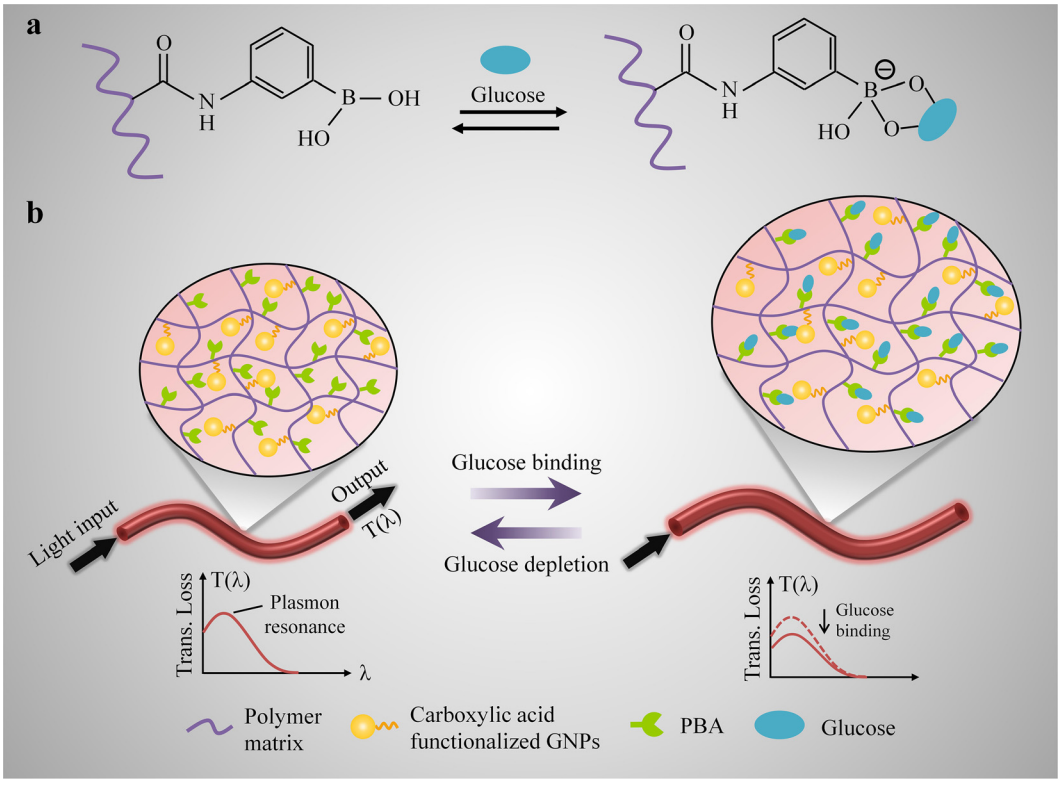

Figure 2: Schematic illustration of the gold nanocomposite hydrogel fiber for glucose detection.
(a) Complexation of 3-(acrylamido)-phenylboronic acid (3-APBA) with cis-diols in glucose molecules. (b) Sensing mechanism. Glucose binding to the hydrogel fiber resulted in volume expansion of the hydrogel matrix, which could be monitored from the change in the light attenuation contributed by the localized surface plasmon resonance (LSPR) effect.

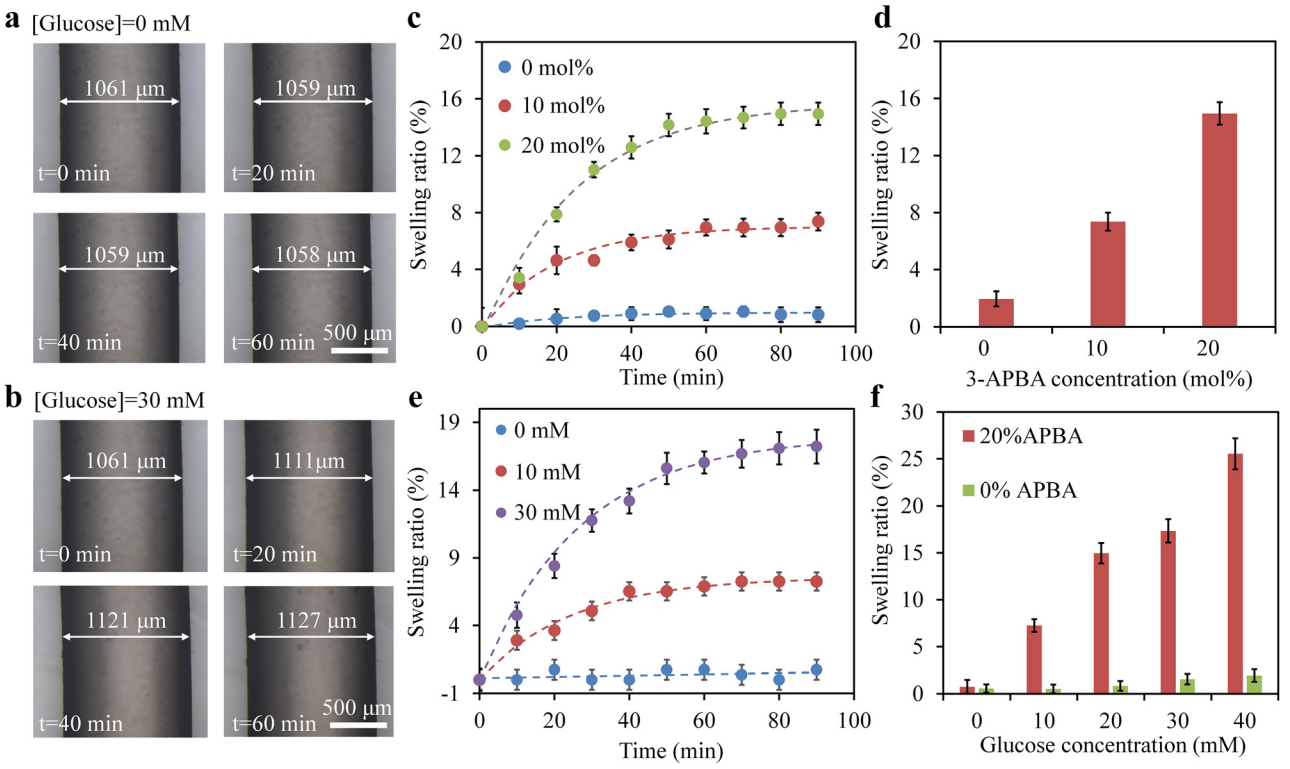

Figure 3: (a, b) Microscope images of the nanocomposite fiber expansion over time under glucose concentrations of 0 mM (a) and 30 mM (b) at pH = 7.4. The concentration of 3-(acrylamido)-phenylboronic acid (3-APBA) was set at 20 mol%. (c) Dependence of 3-APBA concentrations on swelling kinetics of the fibers. (d) Swelling weight ratio of the fibers versus 3-APBA concentration. (e) Swelling kinetics of the fibers under various glucose concentrations. (f) Swelling weight ratio versus glucose concentration for hydrogel fibers with/without 3-APBA functionalization.

measured with time interval of 10 min and continuously recorded for 90 min to reach an equilibrium state. As shown in Figure 3d, the fibers showed increased volumetric shift with the increasing 3-APBA content, indicating a higher glucose sensitivity with more 3-APBA. Considering the limited solubility of 3-APBA in the hydrogel precursor, nanocomposite hydrogel fibers containing 20 mol% 3-APBA were found to be optimum for glucose detection. The swelling responses of the fibers to various glucose concentrations were also investigated (Figure 3e). Increase in the glucose concentration resulted in increased expansion of the functionalized fibers, but did not induce obvious volumetric changes for the fibers without 3-APBA functionalization (Figure 3f). For a high glucose concentration of 40 mM, the functionalized fibers had a swelling weight ratio as large as 25.5%, while the nonfunctionalized fibers only swelled by 1.9%. The selectivity of the fibers was also tested with aqueous samples separately containing $CaCl_2$, KCl, NaCl, glycine, uric acid, ascorbic acid, and glucose (Figure S1, Supplementary information). The fibers showed high selectivity toward glucose due to the specific binding of 3-APBA with cis-diol groups of glucose.

To avoid the GNPs leakage, the GNPs were covalently entrapped within the fiber by using EDC conjunction. The reaction of EDC with the surface carboxyl group on GNPs produced an amine-reactive O-acylisourea intermediate that spontaneously reacted with the amine groups of PAAm, forming a stable amide bond [48]. To confirm the stability and immobilization of the GNPs, the transmission spectra of the nanocomposite fiber over time were recorded in PBS buffer at constant temperature of 26 °C. The LSPR peak wavelength and intensity were indicative of the size and concentration of the GNPs, respectively. As shown in Figure 4a, no shift in the LSPR peak of GNPs was observed in 5 days, suggesting no changes in the particle size. The light attenuation at the resonance peak of the GNPs showed a maximum relative shift of about 0.42 and 0.31 dB over a long-term (5 days) and short-term (60 min) observation period, respectively (Figure 4b,c). These results suggested no leakage of the GNPs from the hydrogel matrix, allowing highly stable optical readout based on LSPR. Due to its high flexibility, the nanocomposite fiber could be bent or twisted with the hosting tissues without mechanical failure, which, however, inevitably induces additional

propagation losses in the fiber. The transmitted attenuation spectra of the fiber under various bending radius were further investigated (Figure 4d,e). The fiber showed increased attenuation over the entire visible wavelength with the decreasing bending radius, which could greatly influence the accuracy of glucose determination. To minimize this effect, a dual-wavelength differential detection method was employed for the sensor readout. Besides the LSPR peak, we chose another reference wavelength (700 nm) out of the plasmon resonance region to offer an internal calibration. Figure 4f shows the bending-dependent light attenuation at 528 and 700 nm, respectively. As the bending radius was decreased to 1 cm, significant light attenuation (>5 dB) were observed at both 528 and 700 nm with similar trend. In contrast, the variation in the differential attenuation of the two wavelengths was below 0.2 dB due to the suppression of the bending-dependent effects.

To show the capability of the nanocomposite fiber sensor for quantifying glucose concentration, we characterized the spectral response of the sensor upon exposure to glucose in a clinically relevant range (0–40 mM) under simulated physiological conditions (PBS buffer, pH = 7.4) (Figure 5a,b). We defined the glucose sensitivity as the magnitude in shift of the differential attenuation per unit change of glucose concentration. As the glucose concentration was increased from 0 to 40 mM, the sensor showed linearly decreased attenuation with correlation coefficients of 0.96 and 0.98, and sensitivities of −0.05 dB/mM and −0.13 dB/mM for low (0.01% w/v) and high (0.02% w/v) doping amounts of GNPs, respectively (Figure 5c). The higher sensitivity achieved with higher loading of GNPs was attributed to the stronger LSPR effect. The detection limit of the sensor at GNPs concentration of 0.02% w/v was estimated to be 0.75 mM (S/N = 3). The temporal response of the fiber sensor for different glucose concentrations were investigated by continuously recording its attenuation spectra (Figure 5d). The sensor exhibited stable optical readout over time in the absence of glucose. Upon addition of glucose, the sensor showed rapid response and reached binding equilibrium in 50 min, which provided a readout rate of 0.6 mM·min^{-1}, much higher than the required speed for diabetic patients (0.078 mM·min^{-1} [34]). The reusability of the sensor was evaluated by a cycling test of glucose

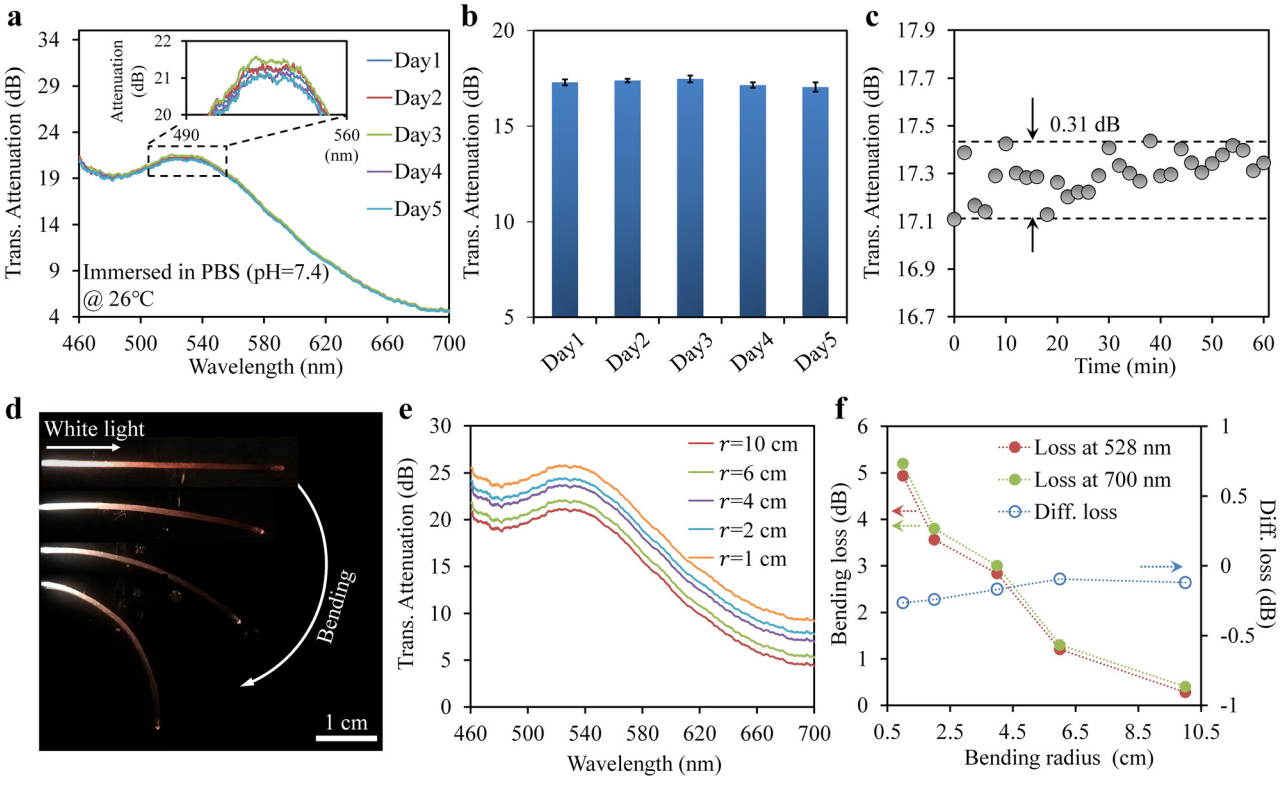

Figure 4: (a) Time-lapse transmission spectra of the nanocomposite fiber in phosphate-buffered saline (PBS) buffer at 26 °C. b, c) Changes of light attenuation at the resonance peak (528 nm) of gold nanoparticles (GNPs) over a long-term (b) and short-term (c) observation period. (d) Photograph showing a nanocomposite fiber applied with gradually decreased bending radius. (e) Transmission spectra of the fiber under various bending radius. (f) Bending loss of the fiber at 528 and 700 nm (left axis), and the differential loss (right axis).

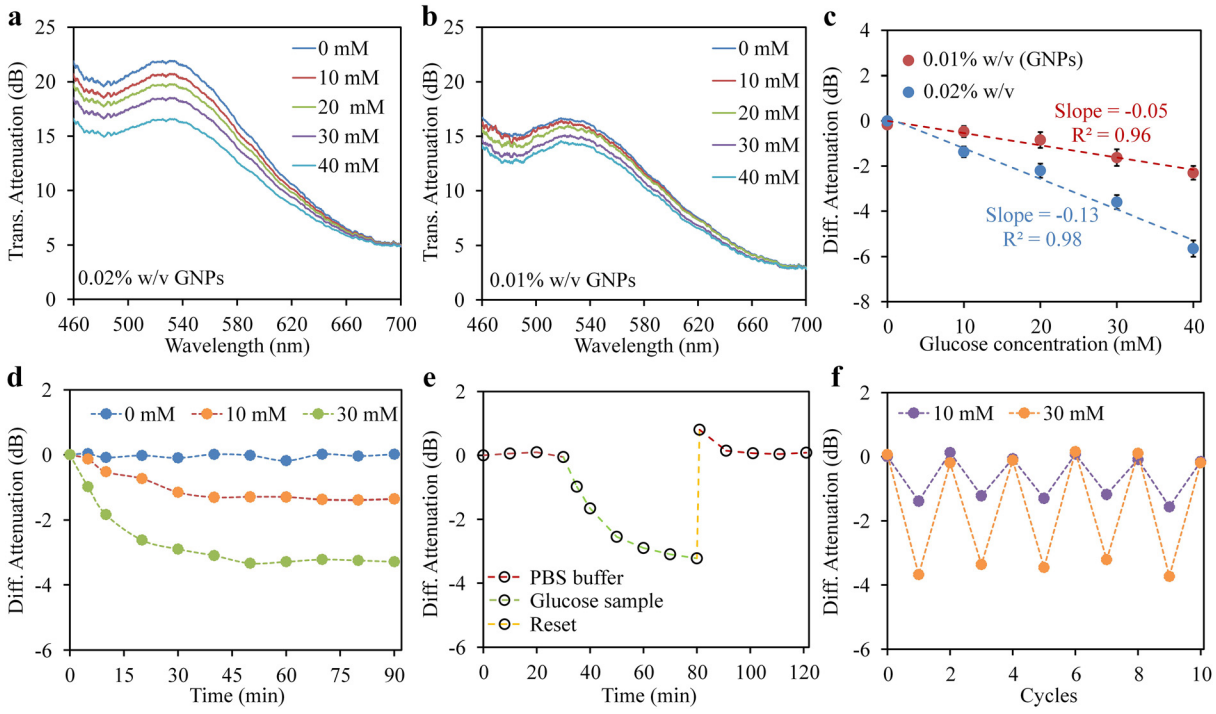

Figure 5: (a, b) Spectral response of the fiber sensors in different glucose concentrations (0–40 mM). The doping amounts of gold nanoparticles (GNPs) in (a) and (b) were 0.02% and 0.01% w/v, respectively. (c) Differential light attenuation at 528 and 700 nm versus glucose concentration. (d) Temporal response of the sensor to various glucose concentration. (e) Reusability of the sensor. (f) Response of the sensor to repeated cycles of glucose binding and releasing under glucose concentrations of 10 and 30 mM.

binding and releasing, where the sensor was first treated with glucose solution (30 mM) for 50 min, and then reset by an acetate buffer (pH 4.6) for 1 min to release the bond glucose molecules (Figure 5e). When immersed in PBS buffer after the reset, the sensor readout recovered to its initial value. Figure 5f shows the response of the sensor to repeated glucose cycles, where the sensor readout was reproducible during each cycle with negligible hysteresis. These results demonstrate stable and reliable performances of the sensor for glucose quantification with high sensitivity and reusability under physiological conditions.

The influence of temperature variation on the sensor response was studied within the range of 24–51 °C (Figure S2a,b). As the temperature increased, the sensor showed significantly decreased attenuation due to swelling of the hydrogel matrix, caused by the disentanglement of interpenetrated polymeric chains and destruction of molecular hydrogen bonding [49]. The attenuation readout shifted by 3.4 dB as the temperature increased to 51 °C. GNPs-loaded hydrogels have been intensively investigated for photothermal studies based on plasmonic heating [35–39]. As the hydrogel sensor herein was interrogated by low-energy white light source, negligible heating effect was observed during the sensor operation (temperature changes: <1 °C). Furthermore, the effect of pH on the sensor readout was investigated by immersing the sensor in buffer solutions of various pH at constant temperature of 26 °C (Figure S3a,b). The sensor maintained a stable readout within the pH range of 4.6–6, indicating negligible change in its volume. However, as the pH increased above 6, a considerable increase in the hydrogel swelling was found due to the increased anionic boronate ions, leading to significant decrease (as large as 4.3 dB at pH 10.5) in the sensor output. Due to the strong temperature and pH dependences, the sensor should be calibrated against different application environments. To further confirm its utility in human biological samples, we tested the sensor with commercially available human blood serum. The sensor was immersed in serum samples spiked with standard glucose concentrations of 5, 10, 15 mM, respectively, at normal body temperature (37 °C) (Table S1). Each serum sample was tested three times. The recoveries of the samples were found to be 98.7–106%, and the relative standard deviation (RSD) was in the range of 2.8–5.4%, which validated the reproducibility and accuracy of the sensor for glucose detection in practical utility.

3 Conclusions

In summary, we have demonstrated a soft and flexible optical glucose sensor based on GNPs-incorporated hydrogel optical fiber, which offers excellent optical and physio-mechanical properties suitable for implantable glucose monitoring. To avoid the leakage of the GNPs from the fiber, the GNPs were modified with carboxylic acid and covalently attached onto the hydrogel matrix through EDC conjugation. For glucose sensing, the fiber was functionalized with 3-APBA, which can bind with cis-diols in glucose molecules, increasing the osmotic Donnan pressure, and consequently resulting in volumetric changes of the fiber. This glucose-dependent volumetric shift could be monitored from the change in light attenuation contributed by LSPR of the incorporated GNPs for glucose quantification. Readout of the optical sensor from light transmission was susceptible to the loss effect associated with fiber bending. This was minimized by a dual-wavelength differential approach, which employed a reference wavelength to offer an internal calibration. Quantitative characterizations of the sensor showed a linear response in the clinically relevant range of 0–40 mM with high sensitivity (−0.13 dB/mM) and fast responsitivity (0.6 mM·min^{-1}) under physiological conditions. Furthermore, the sensor showed reversible and reproducible responses over repeated testing cycles at different glucose levels with negligible hysteresis. The presented optical sensor may find applications in wearable and implantable continuous glucose monitoring at point-of-care settings. Harnessing this sensor concept, it is also possible to realize biosensors for detection of other bioanalytes.

4 Methods

4.1 Fabrication of the nanocomposite fiber glucose sensor

Acrylamide (AAm), *N*,*N*′-methylenebis(acrylamide) (BIS), 3-(acrylamido) phenylboronic acid (3-APBA), diethoxyacetophenone (DEAP), phosphate-buffered saline (PBS) buffer (pH 7.4, ionic strength 150 mM), dimethyl sulfoxide (DMSO), D-(+)-glucose, Tris HCl, Tris base, and *N*-(3-dimethylaminopropyl)-*N*′-ethylcarbodiimide hydrochloride (EDC) were purchased from Sigma-Aldrich and used without further purification. Hydrogel precursor was prepared by mixing AAm (78.5 mol%), BIS (1.5 mol %), 3-APBA (20 mol%) with DEAP (2% w/v) in DMSO (1 mL), followed by monomer dilution with DI water (1 mL). After being carefully degassed, the precursor solution was injected into a polyvinyl chloride (PVC) tube mold (inner diameter: 1 mm) using a syringe adapted with a 0.45 μm filter. Glucose-responsive hydrogel optical fibers were formed by curing the precursor solution under UV exposure (365 nm) for 5 min. To extract the hydrogel fiber from the tube mold, water pressure was applied through syringe injection.

The fiber glucose sensor was fabricated by using glucose-responsive hydrogel fiber incorporating covalently immobilized GNPs. Carboxylic acid-modified GNPs were synthesized following previously reported procedures [50, 51], and the stock solution was utilized for the sensor fabrication. The GNPs (0–0.02% w/v) were doped into the hydrogel fibers through precursor mixing, followed by UV polymerization for 5 min. Afterward, the gold nanocomposite hydrogel fibers were treated with EDC for 9 h at pH 4.5. The resulting fibers were rinsed with DI water and kept in PBS buffer at pH 7.4.

4.2 Equipment and characterization

The microscopic image of the GNPs was taken by a 120 kV transmission electron microscope (TEM, Tecnai Spirit). Mechanical characterization of the hydrogels fibers was performed by using a tensile tester with a 500 N load cell (Handpi Instrumnets). Transmission spectra of the hydrogel fibers were measured with a compact spectrometer (Ocean optics, Maya 2000) equipped with a halogen light source (Ocean optics, HL-2000). The temperature-dependent effect of the fiber sensor was evaluated by using a thermocouple (resolution, 0.1 °C) and heating tape. For pH titration experiments, Tris HCl and Tris base were used to prepare pH buffers (pH 4.6–10.5, ionic strength 150 mM). The stability test was performed by immersing the fiber sensor in PBS buffer at 26 °C, during which no agitation was applied.

4.3 Glucose sensing experiments

The nanocomposite fiber sensor was integrated with silica multimode fiber (MMF) for light coupling. PBS buffer solutions (pH 7.4, ionic strength 150 mM) were used to prepare glucose samples with concentrations ranging from 0 to 40 mM. Prior to the glucose testing, the fiber sensor was immersed in a Petri dish containing PBS buffer (glucose-free) and allowed to be fully swollen at 26 °C. To investigate the glucose response of the sensor, the blank PBS buffer was replaced by glucose sample at a selected concentration, and the optical transmissions of the nanocomposite fiber were continuously recorded by a fiber-coupled spectrometer. To evaluate the reusability, the sensor was reset in acetate buffer (pH 4.6) for 2 min to release the bond glucose molecules and then immersed in PBS buffer for 30 min before commencing the next glucose test.

Acknowledgments: J.G. acknowledges the funding from the National Natural Science Foundation of China (No. 61805126, 62175008). L.K. acknowledges the support from the "Thousand Talents Plan" Youth Program of China.
Author contribution: J.G. and L.K. conceived the idea. J.G. and B.Z. performed the experiments. J.G., L.K., and B.Z. analyzed the data. All authors contributed to the editing of the manuscript.
Research funding: None declared.
Conflict of interest statement: The authors declare no conflicts of interest regarding this article.

Data availability: The data that support the findings of this study are available from the corresponding author upon request.

References

[1] C. Chen, Q. Xie, D. Yang, et al., "Recent advances in electrochemical glucose biosensors: a review," *RSC Adv.*, vol. 3, p. 4473, 2013.

[2] S. K. Vashist, D. Zheng, K. Al-Rubeaan, J. H. Luong, and F. S. Sheu, "Technology behind commercial devices for blood glucose monitoring in diabetes management: a review," *Anal. Chim. Acta*, vol. 703, p. 124, 2011.

[3] J. A. Usher-Smith, M. J. Thompson, S. J. Sharp, and F. M. Walter, "Factors associated with the presence of diabetic ketoacidosis at diagnosis of diabetes in children and young adults: a systematic review," *BMJ*, vol. 343, p. d4092, 2011.

[4] L. Olansky and L. Kennedy, "Finger-stick glucose monitoring: issues of accuracy and specificity," *Diabetes Care*, vol. 33, p. 948, 2010.

[5] V. R. Kondepati and H. M. Heise, "Recent progress in analytical instrumentation for glycemic control in diabetic and critically ill patients," *Anal. Bioanal. Chem.*, vol. 388, p. 545, 2007.

[6] M. Vettoretti and A. Facchinetti, "Combining continuous glucose monitoring and insulin pumps to automatically tune the basal insulin infusion in diabetes therapy: a review," *Biomed. Eng. Online*, vol. 18, p. 37, 2019.

[7] D. Chen, C. Wang, W. Chen, Y. Chen, and J. X. Zhang, "PVDF-Nafion nanomembranes coated microneedles for in vivo transcutaneous implantable glucose sensing," *Biosens. Bioelectron.*, vol. 74, p. 1047, 2015.

[8] S. A. Zaidi and J. H. Shin, "Recent developments in nanostructure based electrochemical glucose sensors," *Talanta*, vol. 149, p. 30, 2016.

[9] J. Zhang, X. Yu, W. Guo, et al., "Construction of titanium dioxide nanorod/graphite microfiber hybrid electrodes for a high performance electrochemical glucose biosensor," *Nanoscale*, vol. 8, p. 9382, 2016.

[10] Y. J. Heo, H. Shibata, T. Okitsu, T. Kawanishi, and S. Takeuchi, "Long-term in vivo glucose monitoring using fluorescent hydrogel fibers," *Proc. Natl. Acad. Sci. USA*, vol. 108, p. 13399, 2011.

[11] D. Rodbard, "Continuous glucose monitoring: a review of successes, challenges, and opportunities," *Diabetes Technol. Therapeut.*, vol. 18, p. S2, 2016.

[12] M. Elsherif, M. U. Hassan, A. K. Yetisen, and H. Butt, "Wearable contact lens biosensors for continuous glucose monitoring using smartphones," *ACS Nano*, vol. 12, p. 5452, 2018.

[13] M. J. Yin, B. Gu, Q. F. An, C. Yang, Y. L. Guan, and K. T. Yong, "Recent development of fiber-optic chemical sensors and biosensors: mechanisms, materials, micro/nano-fabrications and applications," *Coord. Chem. Rev.*, vol. 376, p. 348, 2018.

[14] S. Novais, C. I. Ferreira, M. S. Ferreira, and J. L. Pinto, "Optical fiber tip sensor for the measurement of glucose aqueous solutions," *IEEE Photonics J.*, vol. 10, p. 1, 2018.

[15] S. Tierney, S. Volden, and B. T. Stokke, "Glucose sensors based on a responsive gel incorporated as a Fabry-Perot cavity on a fiber-optic readout platform," *Biosens. Bioelectron.*, vol. 24, p. 2034, 2009.

[16] S. W. Harun, A. A. Jasim, H. A. Rahman, M. Z. Muhammad, and H. Ahmad, "Micro-ball lensed fiber-based glucose sensor," *IEEE Sensor. J.*, vol. 13, p. 348, 2012.

[17] K. C. Liao, T. Hogen-Esch, F. J. Richmond, L. Marcu, W. Clifton, and G. E. Loeb, "Percutaneous fiber-optic sensor for chronic glucose monitoring in vivo," *Biosens. Bioelectron.*, vol. 23, p. 1458, 2008.

[18] S. Yu, L. Ding, H. Lin, W. Wu, and J. Huang, "A novel optical fiber glucose biosensor based on carbon quantum dots-glucose oxidase/cellulose acetate complex sensitive film," *Biosens. Bioelectron.*, vol. 146, p. 111760, 2019.

[19] S. Singh and B. D. Gupta, "Fabrication and characterization of a surface plasmon resonance based fiber optic sensor using gel entrapment technique for the detection of low glucose concentration," *Sensor. Actuator. B Chem.*, vol. 177, p. 589, 2013.

[20] H. Yuan, W. Ji, S. Chu, et al., "Fiber-optic surface plasmon resonance glucose sensor enhanced with phenylboronic acid modified Au nanoparticles," *Biosens. Bioelectron.*, vol. 117, p. 637, 2018.

[21] Y. Yuan, X. Yang, D. Gong, et al., "Investigation for terminal reflection optical fiber SPR glucose sensor and glucose sensitive membrane with immobilized GODs," *Opt. Express*, vol. 25, p. 3884, 2017.

[22] S. P. Nichols, A. Koh, W. L. Storm, J. H. Shin, and M. H. Schoenfisch, "Biocompatible materials for continuous glucose monitoring devices," *Chem. Rev.*, vol. 113, p. 2528, 2013.

[23] S. Vaddiraju, D. J. Burgess, I. Tomazos, F. C. Jain, and F. Papadimitrakopoulos, "Technologies for continuous glucose monitoring: current problems and future promises," *J. Diabetes Sci. Technol.*, vol. 4, p. 1540, 2010.

[24] J. Guo, C. Yang, Q. Dai, and L. Kong, "Soft and stretchable polymeric optical waveguide-based sensors for wearable and biomedical applications," *Sensors*, vol. 19, p. 3771, 2019.

[25] S. Shabahang, S. Kim, and S. H. Yun, "Light-guiding biomaterials for biomedical applications," *Adv. Funct. Mater.*, vol. 28, p. 1706635, 2018.

[26] R. Nazempour, Q. Zhang, R. Fu, and X. Sheng, "Biocompatible and implantable optical fibers and waveguides for biomedicine," *Materials*, vol. 11, p. 1283, 2018.

[27] J. Guo, X. Liu, N. Jiang, et al., "Highly stretchable, strain sensing hydrogel optical fibers," *Adv. Mater.*, vol. 28, p. 10244, 2016.

[28] J. Feng, Y. Zheng, S. Bhusari, M. Villiou, S. Pearson, and A. del Campo, "Printed degradable optical waveguides for guiding light into tissue," *Adv. Funct. Mater.*, vol. 30, p. 2004327, 2020.

[29] M. Choi, M. Humar, S. Kim, and S. H. Yun, "Step-index optical fiber made of biocompatible hydrogels," *Adv. Mater.*, vol. 27, p. 4081, 2015.

[30] J. Guo, H. Huang, M. Zhou, C. Yang, and L. Kong, "Quantum dots-doped tapered hydrogel waveguide for ratiometric sensing of metal ions," *Anal. Chem.*, vol. 90, p. 12292, 2018.

[31] J. Guo, Y. Luo, C. Yang, and L. Kong, "In situ surface-enhanced Raman scattering sensing with soft and flexible polymer optical fiber probes," *Opt. Lett.*, vol. 43, p. 5443, 2018.

[32] R. Kumar, A. P. Singh, A. Kapoor, and K. N. Tripathi, "Effect of dye doping in poly (vinyl alcohol) waveguides," *J. Mod. Opt.*, vol. 52, p. 1471, 2005.

[33] L. Wang, C. Zhong, D. Ke, et al., "Ultrasoft and highly stretchable hydrogel optical fibers for in vivo optogenetic modulations," *Adv. Opt. Mater.*, vol. 6, p. 1800427, 2018.
[34] J. Feng, Q. Jiang, P. Rogin, P. W. de Oliveira, and A. Del Campo, "Printed soft optical waveguides of PLA copolymers for guiding light into tissue," *ACS Appl. Mater. Interfaces*, vol. 12, p. 20287, 2020.
[35] C. Wang, X. Liu, V. Wulf, M. Vázquez-González, M. Fadeev, and I. Willner, "DNA-based hydrogels loaded with Au nanoparticles or Au nanorods: thermoresponsive plasmonic matrices for shape-memory, self-healing, controlled release, and mechanical applications," *ACS Nano*, vol. 13, p. 3424, 2019.
[36] E. Castellanos, B. Soberats, S. Bujosa, C. Rotger, R. de la Rica, and A. Costa, "Development of plasmonic Chitosan–Squarate hydrogels via bioinspired nanoparticle growth," *Biomacromolecules*, vol. 21, p. 966, 2019.
[37] L. Moretti, A. Mazzanti, A. Rossetti, et al., "Plasmonic control of drug release efficiency in agarose gel loaded with gold nanoparticle assemblies," *Nanophotonics*, vol. 10, p. 247, 2021.
[38] I. Vassalini, G. Ribaudo, A. Gianoncelli, M. F. Casula, and I. Alessandri, "Plasmonic hydrogels for capture, detection and removal of organic pollutants," *Environ. Sci. Nano*, vol. 7, p. 3888, 2020.
[39] S. C. Moorcroft, L. Roach, D. G. Jayne, Z. Y. Ong, and S. D. Evans, "Nanoparticle-loaded hydrogel for the light-activated release and photothermal enhancement of antimicrobial peptides," *ACS Appl. Mater. Interfaces*, vol. 12, p. 24544, 2020.
[40] C. L. Shen, Q. Lou, J. H. Zang, et al., "Near-infrared chemiluminescent carbon nanodots and their application in reactive oxygen species bioimaging," *Adv. Sci.*, vol. 7, p. 1903525, 2020.
[41] C. L. Shen, Q. Lou, K. K. Liu, L. Dong, and C. X. Shan, "Chemiluminescent carbon dots: synthesis, properties, and applications," *Nano Today*, vol. 35, p. 100954, 2020.
[42] C. L. Shen, G. S. Zheng, M. Y. Wu, et al., "Chemiluminescent carbon nanodots as sensors for hydrogen peroxide and glucose," *Nanophotonics*, vol. 9, p. 3597, 2020.
[43] A. K. Yetisen, N. Jiang, A. Fallahi, et al., "Glucose-sensitive hydrogel optical fibers functionalized with phenylboronic acid," *Adv. Mater.*, vol. 29, p. 1606380, 2017.
[44] G. Chen, N. Matsuhisa, Z. Liu, et al., "Plasticizing silk protein for on-skin stretchable electrodes," *Adv. Mater.*, vol. 30, p. 1800129, 2018.
[45] P. Antunes, H. Lima, J. Monteiro, and P. S. André, "Elastic constant measurement for standard and photosensitive single mode optical fibres," *Microw. Opt. Technol. Lett.*, vol. 50, p. 2467, 2008.
[46] U. Klueh, M. Kaur, D. C. Montrose, and D. L. Kreutzer, "Inflammation and glucose sensors: use of dexamethasone to extend glucose sensor function and life span in vivo," *J. Diabetes Sci. Technol.*, vol. 1, p. 496, 2007.
[47] M. Elsherif, M. U. Hassan, A. K. Yetisen, and H. Butt, "Glucose sensing with phenylboronic acid functionalized hydrogel-based optical diffusers," *ACS Nano*, vol. 12, p. 2283, 2018.
[48] Y. Lei, H. Tang, C. Zhou, T. Zhang, M. Feng, and B. Zou, "Incorporating fluorescent quantum dots into water-soluble polymer," *J. Lumin.*, vol. 128, p. 277, 2008.
[49] N. V. Gupta and H. G. Shivakumar, "Investigation of swelling behavior and mechanical properties of a pH-sensitive superporous hydrogel composite, *Iran*," *J. Pharm. Res.*, vol. 11, p. 481, 2012.
[50] S. Sabouri, H. Ghourchian, M. Shourian, and M. Boutorabi, "A gold nanoparticle-based immunosensor for the chemiluminescence detection of the hepatitis B surface antigen," *Anal. Methods.*, vol. 6, p. 5059, 2014.
[51] M. H. Jazayeri, H. Amani, A. A. Pourfatollah, H. Pazoki-Toroudi, and B. Sedighimoghaddam, "Various methods of gold nanoparticles (GNPs) conjugation to antibodies," *Sens. Biosensing Res.*, vol. 9, p. 17, 2016.

Supplementary Material: The online version of this article offers supplementary material (https://doi.org/10.1515/nanoph-2021-0360).